

## Supplementary Information

### **Strongly Anisotropic Optoelectronic Properties and Long Exciton Lifetimes in Two-Dimensional GaInS<sub>3</sub>-Type Monolayers**

*Nian Zhang*<sup>1,2</sup>, *Wangping Xu*<sup>1,3\*</sup>, *Li Xiang*<sup>1</sup>, *Ziwei Zhao*<sup>1</sup>, *Juexian Cao*<sup>1,3</sup>, and  
*Xiaolin Wei*<sup>1,2\*</sup>

<sup>1</sup> *Department of Physics & Hunan Institute of Advanced Sensing and Information  
Technology, Xiangtan University, Xiangtan 411105, People's Republic of China*

<sup>2</sup> *College of Physics and Electronics Engineering, Hengyang Normal University,  
Hengyang 421002, People's Republic of China*

<sup>3</sup> *Hunan Provincial Key Laboratory of Smart Carbon Materials and Advanced Sensing,  
Xiangtan University, Xiangtan 411105, People's Republic of China*

\*E-mail: [xuwp@xtu.edu.cn](mailto:xuwp@xtu.edu.cn); [xlw@xtu.edu.cn](mailto:xlw@xtu.edu.cn)

## Supplementary Figures

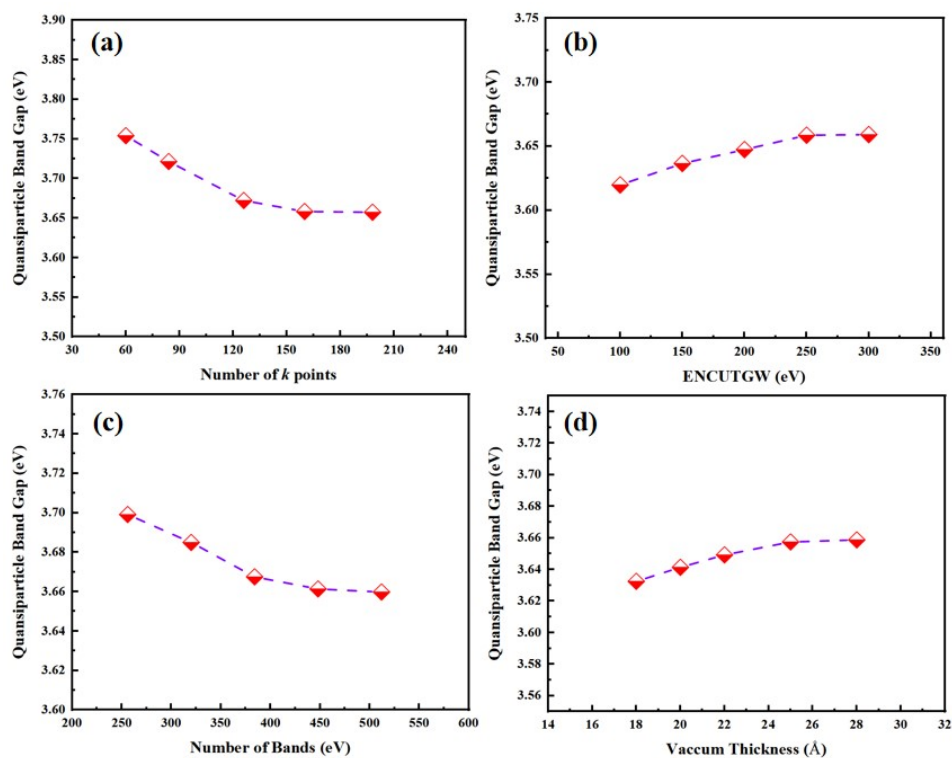


**Figure S1.** Convergence tests of the quasiparticle band gap of  $\alpha$ -GaInS<sub>3</sub> monolayer with respect to (a)  $k$ -point numbers, (b) GW cutoff energy, (c) the number of bands, and (d) the vacuum thickness.

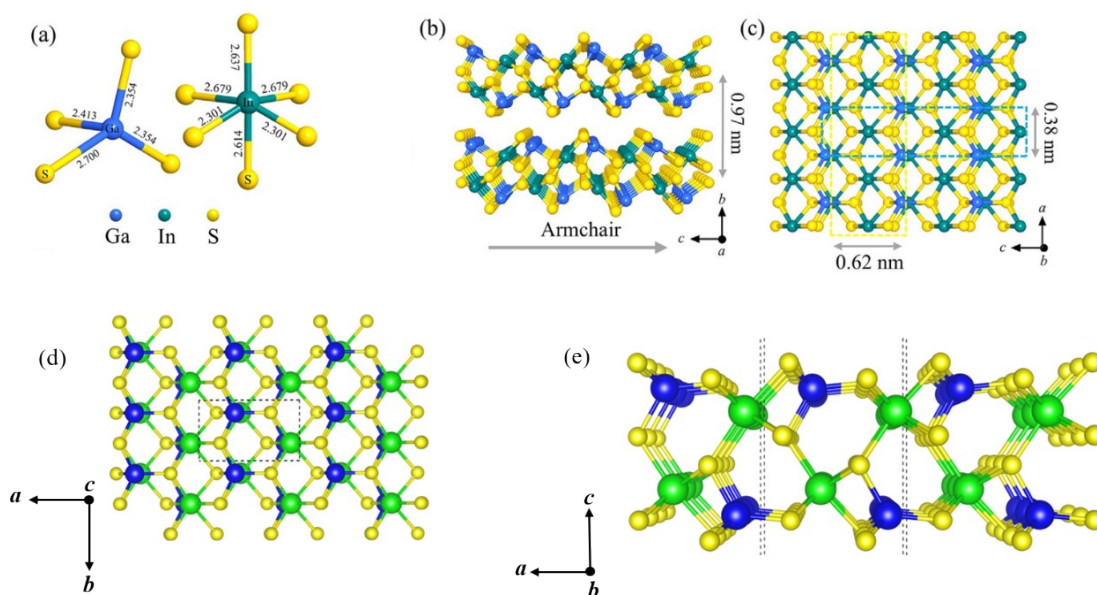


**Figure S2.** (a) The two structural units comprising GaS<sub>4</sub> tetrahedra and InS<sub>6</sub> octahedra within GaInS<sub>3</sub>; (b) a side view of the bilayer GaInS<sub>3</sub> structure; and (c) a top view. (d) Top view of a single-

layer  $\alpha$ -GaInS<sub>3</sub> structure and (e) side view.

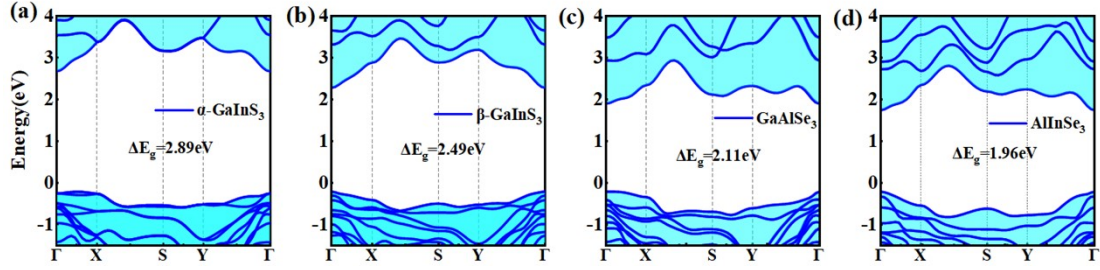


**Figure S3.** (a) Band structure diagram of  $\alpha$ -GaInS<sub>3</sub> in the HSE06 model. (b-d) Band structure diagrams of three direct-bandgap variants of HSE06 in the ABM<sub>3</sub> model.

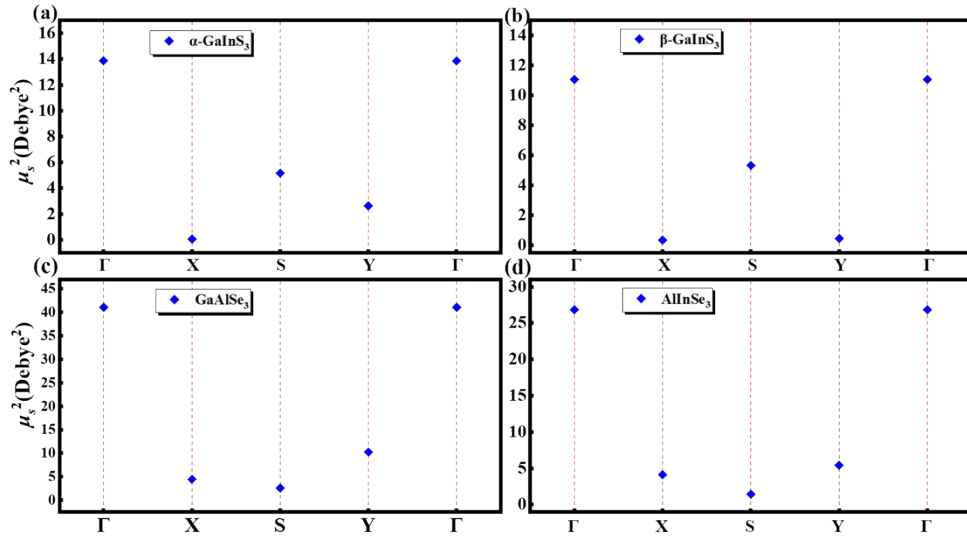


**Figure S4.** Calculated exciton dipole moments of GaInS<sub>3</sub>-like rectangular monolayers (a)  $\alpha$ -GaInS<sub>3</sub> (b)  $\beta$ -GaInS<sub>3</sub> (c) GaAlSe<sub>3</sub> and (d) AlInSe<sub>3</sub>.

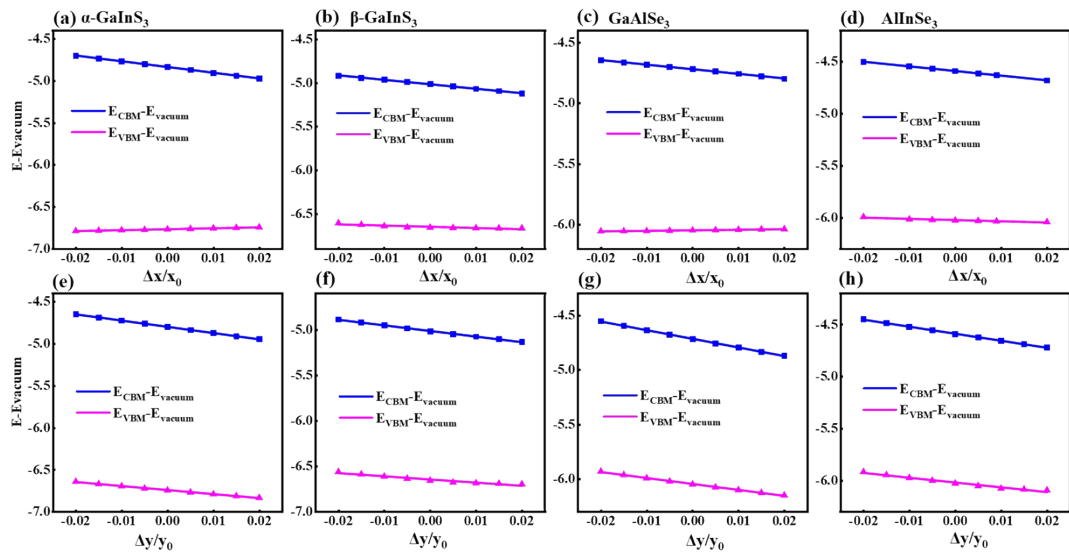


**Figure S5.** (a-d) Formation energies of the experimental  $\alpha$ -GaInS<sub>3</sub> structure and ABM<sub>3</sub>

structure along the x-direction. (e–h) Formation energies of the experimental  $\alpha$ -GaInS<sub>3</sub> structure and ABM<sub>3</sub> structure along the y-direction.

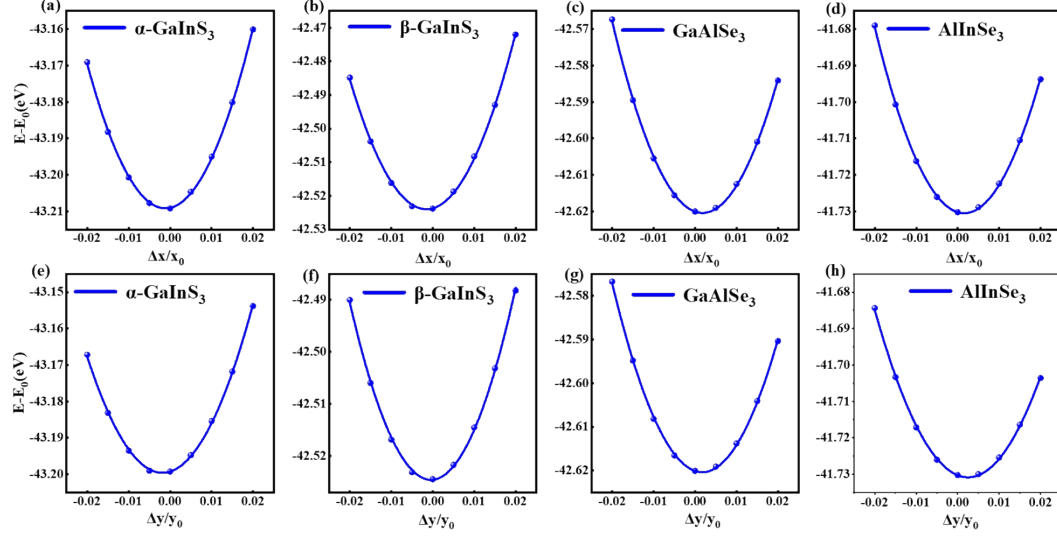


**Figure S6.** (a–d) Experimental  $\alpha$ -GaInS<sub>3</sub> structures and ABM<sub>3</sub> structures: elastic modulus ( $C_{2D}$ ) images along the x-direction. (e–h) Experimental  $\alpha$ -GaInS<sub>3</sub> structures and ABM<sub>3</sub> structures: elastic modulus ( $C_{2D}$ ) images along the y-direction.

**Table S1.** The calculated elastic constants of the three single-layer materials.

| Elastic constant        | $\beta$ -GaInS <sub>3</sub> | GaAlSe <sub>3</sub> | AlInSe <sub>3</sub> |
|-------------------------|-----------------------------|---------------------|---------------------|
| $C_{11}$                | 45.52                       | 48.08               | 41.09               |
| $C_{12}$                | 10.34                       | 9.45                | 9.15                |
| $C_{22}$                | 34.16                       | 36.72               | 31.95               |
| $C_{66}$                | 8.21                        | 9.97                | 8.85                |
| $C_{11}C_{22}-C_{12}^2$ | 1448.25                     | 1676.20             | 1229.10             |

### **Carrier Mobility calculation**

To investigate the material electron and hole transport properties, here, we use the phonon-limited scattering model of the deformation potential theory proposed by Bardeen and Shockley to predict the carrier mobility of monolayer ABM<sub>3</sub> (A=Ga, In, Al; B=Ga, In, Al; M=S, Se, Te). For the 2D semiconductor system, we used the following equation to calculate the intrinsic carrier mobility of the monolayers<sup>[1,2]</sup>:

$$\mu_{2D} = \frac{eh^3 C_{2D}}{K_B T m^* m_d E_l^2} \quad (1)$$

where  $T$ ,  $m^*$ ,  $C_{2D}$ ,  $E_l$ ,  $K_B$  are the temperature, the effective masses of electrons and holes, the elastic modulus of a uniformly deformed crystal, the variational constant along the transport direction, and the Boltzmann constant, respectively.  $m^*$  depends on the energy change of the wave vector  $k$  along different transport directions, defined as

$$m^* = \frac{\hbar^2}{(\partial^2 E / \partial^2 k)}$$

$m_d$  is the average effective mass, which is determined

$m_d = \sqrt{m_x m_y}$ . The valence band maximum (VBM) of electrons along the transport direction or the conduction band minimum (CBM) of the deformation situation constant

$$E_l, \text{ determined by } E_x = \frac{\Delta E_{lx}}{(\Delta l_x / l_{x0})} \text{ and } E_y = \frac{\Delta E_{ly}}{(\Delta l_y / l_{y0})}.$$

The calculation of the deformation potential  $C_{2D}$  and the distortion potential  $E_l$  in the paper is based on the equilibrium lattice structure, respectively, along with the uniaxial axis of the in-plane cell or by applying different values of stretching and compression in the interval from -2% to 2% (taking a series of discrete values at 0.5% intervals) to achieve the calculation of the cell under different strains.

### **References:**

- [1] J. Bardeen, W. Shockley, Deformation potentials and mobilities in non-polar crystals, Phys. Rev., 80(1950) 72-80.
- [2] J. Qiao, X. Kong, Z. Hu, F. Yang, W. Ji, High-mobility transport anisotropy and linear dichroism in few-layer black phosphorus, Nat. Commun., 5(2014) 4475.

